Review Article

Challenges in clinical translation of cardiac magnetic resonance imaging radiomics in non-ischemic cardiomyopathy: a narrative review

Jia Deng[1#], Langtao Zhou[2#^], Bihong Liao[1#], Qinxi Cai[1], Guanghua Luo[1*], Hong Zhou[1*^], Huifang Tang[3*]

[1]The First Affiliated Hospital, Department of Radiology, Hengyang Medical School, University of South China, Hengyang, China; [2]The School of Optics and Photonics, Beijing Institute of Technology, Beijing, China; [3]The First Affiliated Hospital, Department of Cardiology, Hengyang Medical School, University of South China, Hengyang, China

Contributions: (I) Conception and design: J Deng, H Zhou; (II) Administrative support: G Luo, H Tang; (III) Provision of study materials or patients: G Luo, H Zhou; (IV) Collection and assembly of data: J Deng, B Liao; (V) Data analysis and interpretation: J Deng, L Zhou, Q Cai; (VI) Manuscript writing: All authors; (VII) Final approval of manuscript: All authors.

#These authors contributed equally to this work as co-first authors.

*These authors contributed equally to this work.

Correspondence to: Huifang Tang, MD. The First Affiliated Hospital, Department of Cardiology, Hengyang Medical School, University of South China, No. 69 Chuanshan Road, Hengyang 421001, China. Email: tanghuifang999@163.com; Guanghua Luo, MB; Hong Zhou, MD. The First Affiliated Hospital, Department of Radiology, Hengyang Medical School, University of South China, No. 69 Chuanshan Road, Hengyang 421001, China. Email: 1579839814@qq.com; hongzhou@usc.edu.cn.

Background and Objective: Radiomics is an emerging technology that facilitates the quantitative analysis of multi-modal cardiac magnetic resonance imaging (MRI). This study aims to introduce a standardized workflow for applying radiomics to non-ischemic cardiomyopathies, enabling clinicians to comprehensively understand and implement this technology in clinical practice.

Methods: A computerized literature search (up to August 1, 2024) was conducted using PubMed to identify relevant studies on the roles and workflows of radiomics in non-ischemic cardiomyopathy. Expert discussions were also held to ensure the accuracy and relevance of the findings. Only English-language publications were reviewed.

Key Content and Findings: The paper details the essential processes of radiomics, including feature extraction, feature engineering, model construction, and data analysis. It emphasizes the role of MRI in assessing cardiac structure and function and demonstrates how MRI-based radiomics can aid in diagnosing and differentiating non-ischemic cardiomyopathies such as hypertrophic cardiomyopathy, dilated cardiomyopathy, and myocarditis. The study also investigates various cardiac MRI sequences to enhance the clinical application of radiomics.

Conclusions: The standardized radiomics workflow presented in this study aims to assist clinicians in effectively utilizing MRI-based radiomics for the diagnosis and management of non-ischemic cardiomyopathies, thereby improving clinical decision-making.

Keywords: Cardiac magnetic resonance imaging (cardiac MRI); non-ischemic cardiomyopathy; radiomics

Submitted Mar 08, 2024. Accepted for publication Sep 27, 2024. Published online Nov 12, 2024.
doi: 10.21037/cdt-24-138
View this article at: https://dx.doi.org/10.21037/cdt-24-138

^ ORCID: Langtao Zhou, 0000-0002-4290-867X; Hong Zhou, 0000-0002-6460-3420.

Introduction

Background

Cardiac magnetic resonance imaging (MRI) is radiation-free modality with high spatial resolution, enabling the characterization of myocardial structure and tissue (1). Cine sequence in MRI assesses cardiac function, with short-axis and long-axis views facilitating the morphological examination of cardiac anatomical structures. Late gadolinium enhancement (LGE) enables the noninvasive identification of myocardial necrosis and fibrosis, while perfusion is primarily employed to assess myocardial ischemia. Advancements such as T1 mapping, T2 mapping, and feature tracking, are instrumental in detecting diffuse myocardial fibrosis, edema, and cardiac deformational capacity (2,3). Therefore, MRI is essential for assessing cardiac structure, function, myocardial fibrosis, and ischemia, and is indispensable in the diagnosis, risk stratification, and prognosis of cardiomyopathy, myocarditis, and other structural heart diseases (4). However, imaging in multiple planes, parameters, and sequences results in prolonged magnetic resonance (MR) scan times. Due to the complex and varied causes of cardiomyopathy, diagnosing this condition often requires analyzing images from multiple MRI sequences, a task that demands significant clinical expertise (5). Consequently, there is a need to develop new methods to enhance the usability and accessibility of cardiac MRI in clinical practice.

Rationale and knowledge gap

Radiomics, an emerging image analysis technique, extracts a multitude of shapes, textures, and higher-order features from complex clinical imaging data, transforming these into analyzable high-dimensional data. It then identifies radiological features of clinical diagnostic significance, followed by statistical analysis (6,7). For example, radiomics is well established in oncology, in which it is used to determine the probability of benign versus malignant tumors, predict clinical prognostic events, and improve diagnostic, prognostic, and clinical decision support (8). However, its applications in cardiac imaging are still relatively limited. Currently, cardiac imaging primarily utilizes images obtained from computed tomography (CT) and MRI. In CT, its main applications include the evaluation of vulnerable plaques in coronary arteries, and advanced atherosclerotic lesions. In MRI, cardiac radiomics has been independently associated with gender, age, and cardiovascular risk factors in extensive studies involving healthy populations (9,10). Within disease groups, its primary applications lie in structural heart disease, cardiomyopathy, and myocarditis (11). The evolving landscape of cardiac MRI is captured in a recent editorial (12) that delves into the quantitative imaging of the heart and the organs affected by its dysfunction, as well as the growing interest in non-invasive MR methods that eschew contrast enhancement. Cardiac MRI is recognized as the gold standard for diagnosing cardiomyopathies, with radiomics serving as a valuable adjunct in the assessment of cardiac structure and function. Consequently, a comprehensive understanding of the clinical applications and imaging workflows in cardiac MRI histology can markedly enhance the diagnostic precision of clinicians and refine the prediction of clinical outcomes.

Objective

Non-ischemic cardiomyopathies encompass a diverse group of myocardial diseases with varying mechanisms and pathophysiological features. Diagnosing these conditions requires clinicians to synthesize information from multiple sources, including clinical presentation, imaging findings, and histopathology. This complexity poses significant challenges in diagnosis, demanding a high level of clinical expertise. Radiomics, with its ability to extract detailed quantitative features from MRI, offers a promising non-invasive approach to assessing these intricate conditions. This article focuses on the potential of radiomics in non-ischemic cardiomyopathies, aiming to enhance diagnostic accuracy and inform clinical decision-making. It also seeks to familiarize clinicians with the fundamental concepts and workflow of radiomics, while summarizing its current applications in MRI for these diseases. We present this article in accordance with the Narrative Review reporting checklist (available at https://cdt.amegroups.com/article/view/10.21037/cdt-24-138/rc).

Methods

Relevant studies published from January 1, 1973, to August 1, 2024, were retrieved through a comprehensive PubMed search. The search included various combinations of key terms related to cardiovascular magnetic resonance, radiomics, and specific cardiac conditions such as hypertrophic cardiomyopathy (HCM), dilated cardiomyopathy (DCM), and myocarditis. Specific imaging techniques like LGE, T1 mapping, and cine imaging

Table 1 The search terms used

"cardiovascular magnetic resonance" OR "radiomics" AND "hypertrophic cardiomyopathy"
"cardiovascular magnetic resonance" OR "radiomics" AND "dilated cardiomyopathy"
"cardiovascular magnetic resonance" OR "radiomics" AND "myocarditis"
"late gadolinium enhancement" AND "radiomics" AND "hypertrophic cardiomyopathy"
"late gadolinium enhancement" AND "radiomics" AND "dilated cardiomyopathy"
"late gadolinium enhancement" AND "radiomics" AND "myocarditis"
"T1 mapping" OR "native T1" AND "radiomics" AND "hypertrophic cardiomyopathy"
"T1 mapping" OR "native T1" AND "radiomics" AND "dilated cardiomyopathy"
"T1 mapping" OR "native T1" AND "radiomics" AND "myocarditis"
"cine" AND "radiomics" AND "hypertrophic cardiomyopathy"
"cine" AND "radiomics" AND "dilated cardiomyopathy"
"cine" AND "radiomics" AND "myocarditis"

Table 2 The search strategy summary

Items	Specification
Date of search	A second round of literature search up to August 1, 2024
Database searched	PubMed
Search terms used	See *Table 1* for details
Timeframe	January 1, 1973 to August 1, 2024
Inclusion and exclusion criteria	Inclusion: original research articles and reviews in English about radiomics, CMR, and cardiomyopathies. Exclusion: papers with low reliability
Selection process	It was conducted independently by J.D., L.Z., B.L.; data selection is the intersection of the search of three authors
Additional consideration	Additional papers were identified through the review of references in relevant publications

CMR, cardiac magnetic resonance.

were also included. These terms were combined to identify relevant studies exploring the use of radiomics in conjunction with cardiovascular MR for these conditions. A more detailed breakdown of the search terms is provided in *Table 1*. Additional studies were identified through manual reference checks of pertinent articles. Non-English publications and studies of low credibility were excluded. Data extraction focused on the relevance to the research topic rather than a systematic review approach. More details of the search strategy are shown in *Table 2*.

Radiomics workflow

The workflow is depicted in *Figure 1*. *Table 3* provides a detailed illustration of the radiomics workflow in cardiac MRI.

Image acquisition

A prerequisite for radiomics analysis is the acquisition of cardiac images obtained from MRI examinations in patients. This process involves multiple sequences, such as short-axis, long-axis, cine, T1 mapping, T2 mapping, T2-weighted, perfusion, and delayed enhancement. Each cardiac MRI sequence has its own unique role: (I) cine sequences are capable of assessing cardiac morphology and function, but are susceptible to motion and respiratory artefacts; (II) T1 mapping can be used to quantify diffuse myocardial fibrosis, but results are limited by differences in

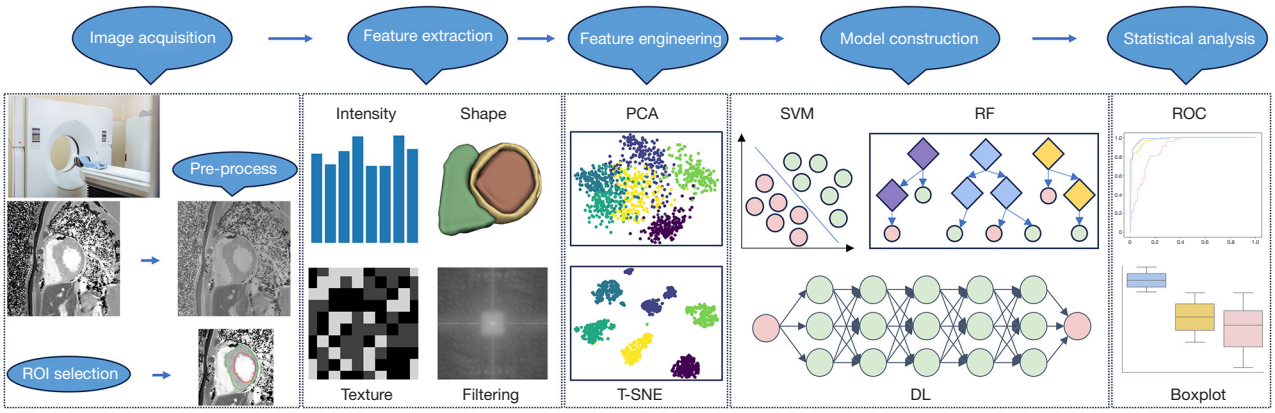

Figure 1 Workflow of radiomics in cardiac MRI. MRI, magnetic resonance imaging; ROI, region of interest; PCA, principal component analysis; T-SNE, T-distributed stochastic neighborhood embedding; SVM, support vector machine; RF, random forest; DL, deep learning; ROC, receiver operating characteristic curve.

equipment, magnetic field strengths and pulse sequences; (III) T2 mapping is effective in detecting oedema, but may lack precision in certain pathological conditions; (IV) stress myocardial perfusion imaging is mainly used to assess myocardial ischemia and coronary reserve function, but there is a risk of inducing myocardial infarction due to vasoconstriction induced by stress agents; (V) LGE is the gold standard for detecting local myocardial fibrosis, but the technique requires the use of a contrast agent and is time-consuming (13).

Figure 2 illustrates the MRI sequences in a patient with HCM. The study received approval from the Review and Ethics Committee of the hospital (No. 2021KS-XN-1202). Informed consent was obtained from the participant. Radiomics can be applied to these multi-sequence cardiac MRI images to extract high-dimensional data for diagnostics, revealing subtle patterns that are not discernible to the human eye. Advanced imaging techniques (14), such as two-dimensional imaging and the application of cardiac and respiratory gating, are frequently employed to enhance image quality by mitigating motion artifacts. This refinement is essential for facilitating precise radiomic analysis.

Image pre-processing

While established guidelines and consensuses aim to standardize cardiac MRI data acquisition protocols (15), the implementation of these standards can vary across institutions, leading to variations in scanning instruments and techniques. Additionally, differences in radiologists' experience and expertise can introduce discrepancies in image interpretation and analysis. These factors contribute to the variability observed in cardiac MRI image (16), emphasizing the importance of harmonization efforts and the continuous refinement of standardized protocols to minimize these differences. Consequently, specific preprocessing operations must be performed the images to ensure data quality and consistency.

Firstly, common issues in cardiac MRI, such as noise and motion artifacts, necessitate image denoising. Denoising techniques can be broadly categorized into traditional methods and those leveraging deep learning. Traditional denoising approaches primarily involve filters [median filtering (17), non-local mean (18), wavelet transform (19), etc.] and other image processing techniques [e.g., sparse representation (20)]. In contrast, deep learning-based techniques, such as those proposed by Zhao *et al.* (21), employ neural networks for automated image denoising and high-quality reconstruction, utilizing generative adversarial networks coupled with super-resolution techniques.

Secondly, the standardization of acquired images (e.g., Z-scoring, aligned coordinate system, resampling) is crucial to ensure data consistency in terms of orientation, resolution, and other parameters. This standardization enables the comparison and combination of different data, enhancing the usability and interpretability of the results. Additionally, image alignment which matches or superimposes images acquired under different conditions, is vital for comparing data across modalities or patients. Moreover, the adoption of generalizable pre-processing

Table 3 Details of radiomics workflow of in cardiac MRI

Steps	Details and some examples
Image acquisition	Include sequences: short-axis, long-axis, cine, T1 mapping, T2 mapping, T2-weighted, perfusion, delayed enhancement
Image pre-processing	
Traditional denoising	Median filtering, non-local mean, sparse representation
Deep learning denoising	Generative adversarial networks
Standardization	Z-scoring, aligned coordinate system, resampling
Generalizable methods	ComBat Harmonization
Region of interest selection	
Traditional methods	Manual mapping, threshold segmentation, region growing, level set
Deep learning	U-Net
Feature extraction	
First-order features	Minimum, maximum, decile, ninetieth, mean, median, interquartile range, standard deviation, root mean square, skewness, kurtosis, variance, uniformity, energy
Shape-based features	Perimeter, area (volume), and diameter
Texture features	Gray level cooccurrence matrix, gray level size zone matrix, gray level run length matrix, neighborhood gray tone difference matrix, gray level dependence matrix
Higher-order features	Edge detection filters (Sobel, Prewitt, Canny), texture filters (Gabor, Haralick, Marr-Hildreth), scale-space filters (Gaussian pyramid), frequency-domain filters (Fourier, wavelet transform)
Feature engineering	
Feature selection	Filtering, packing, embedding
Dimensionality reduction	Principal component analysis, T-distributed stochastic neighborhood embedding
Model construction	
Traditional machine learning	Random forest, support vector machine
Deep learning	Convolutional neural network
Model validation	Metrics (sensitivity, specificity, receiver operating characteristic curve), k-fold cross-validation
Statistical analysis	Descriptive statistical analysis (mean, standard deviation, maximum, minimum values), analysis of variance

MRI, magnetic resonance imaging.

methods such as ComBat Harmonization (22) is imperative, as these techniques have proven effective in ensuring the stability of cardiac MRI-derived radiomic features across varying imaging parameters. Such stabilization is essential for radiomic studies of multi-center datasets.

Region of interest (ROI) selection

ROI selection involves extracting specific anatomical structures or specific areas from cardiac MRI images (23) for further analysis, which are relevant to the study. This process determines the direction and outcomes of subsequent feature extraction and data analysis. Traditional methods include:

(I) Manual mapping is the most traditional method of ROI extraction, where the physician delineates the lesion of interest on the image using a drawing tool via human-computer interaction. This method is typically applied to smaller structures or specific lesion areas, such as the endocardium and epicardium.

(II) Threshold segmentation, such as the Otsu (24), is a commonly used traditional ROI extraction

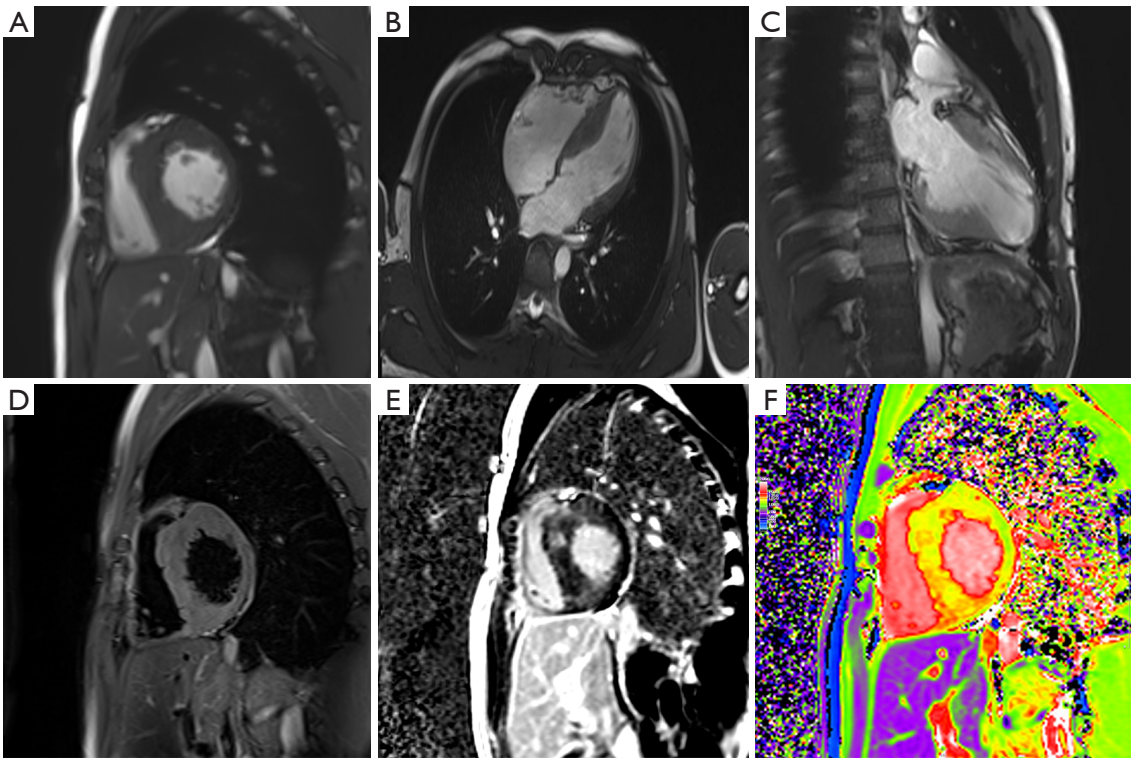

Figure 2 MR scanning sequences in patients with hypertrophic cardiomyopathy: (A) cine short-axis; (B) cine long-axis 4-chambered; (C) cine long-axis 2-chambered; (D) T2WI; (E) late gadolinium enhancement; (F) T1 mapping. MR, magnetic resonance; T2WI, T2-weighted imaging.

technique. It designates pixels in the image with gray values above or below a threshold as ROIs by setting a grayscale threshold. This method is particularly suited to cases with distinct gray values contrasts, such as in the extraction of structures such as tumors and blood vessels.

(III) Region growing (25) is an ROI extraction method that relies on the similarity of pixel gray values. It begins from a seed point and grows the surrounding regions with similar gray values to the seed point until a specific growth criterion is met. This method is more applicable when extracting structures with ambiguous boundaries, such as ventricular wall.

(IV) Other traditional methods include the level set method (26), a technique based on partial differential equation. It converts the image segmentation problem into minimizing an energy function, enabling semi-automatic or fully automatic ROI extraction by extrapolating the ROI boundaries through mathematical equations. This method is advantageous in extracting complex structures, such as the atrial cavity.

Deep learning (27) is an emerging technology that involves training network models to automatically learn and extract ROI from images. This approach performs well on ROI extraction tasks involving large-scale data and complex structures, such as removing myocardial infarction regions (28). These classifications are not mutually exclusive, and some methods can be combined. The selection of the most appropriate ROI extraction method should be based on the characteristics of cardiac MRI images, research objectives, data volume, and the desired level of automation. Additionally, ROI selection should involve choosing representative regions, integrating clinical background and research questions, and ensuring that the selected ROIs are anatomically and physiologically significant.

Feature extraction

In cardiac MRI, feature extraction means transforming information from the ROI into quantitative features.

According to Mayerhoefer *et al.* (29), these features are categorized into first-order, shape-based, texture, and higher-order features. The features defined below are align with those described by Zwanenburg *et al.* (30) and conform to the definitions provided by the Imaging Biomarker Standardization Initiative (31).

First-order features

First-order features analyze a single pixel or voxel based on the global grayscale histogram. The first category includes metrics such as minimum, maximum, decile, ninetieth, mean, median, interquartile range, standard deviation, and root mean square. The second category, which describes the shape of the intensity distribution, includes skewness, kurtosis, variance, and uniformity. Additionally, energy metrics related to the magnitude of pixel or voxel values in the image are included.

Shape-based features

Shape-based features describe the size and shape of the ROI, representing information about the geometric structure of the cardiac anatomy. These features are conceptually straightforward, interpretable, and clinically applicable. Common shape-based features include perimeter, area, and diameter.

- ❖ Perimeter: the number of pixels that border the ROI, used to characterize heart valve contours and identify issues such as leaflet abnormalities or fibrous hyperplasia.
- ❖ Area: measures the dimensions of cardiac structures by evaluating the pixel count within the ROI, providing a direct assessment of heart morphology. It helps assess the size and degree of dilatation in conditions such as myocardial infarction and cardiomyopathy.
- ❖ Diameter: represents the ROI's width, often used to quantify the size of the cardiovascular lumen. Measuring the diameter of the vessels can identify issues such as coronary artery, aortic, and pulmonary artery stenosis.

Texture features

Texture features are commonly utilized for the quantitative characterization of lesions (32). In imaging histology, which mirrors the traditional histological analysis performed with imaging technologies, the characteristic features are commonly extracted through the application of sophisticated computational matrices, categorized according to their respective methods:

- ❖ Gray level cooccurrence matrix (GLCM): describes the relationship between a pixel's gray level and that of its neighboring pixels. Haralick *et al.* (33) proposed 14 statistics based on the GLCM, including energy, entropy, contrast, uniformity, correlation, variance, sum mean, sum variance, entropy, difference variance, difference mean, difference entropy, relevant information measure, and maximum correlation coefficient. These metrics offer diverse perspectives on an image's texture characteristics, such as uniformity (texture thickness), entropy (complexity), and contrast (clarity).
- ❖ Gray level size zone matrix (GLSZM) (34): assess the distribution of zones formed by pixels of the same gray level in an image, characterizing texture features, and the distribution of gray levels.
- ❖ Gray level run length matrix (GLRLM) (35): focuses on the continuity of gray levels or gray values in an image by calculating the run length and distribution of consecutively occurring pixels with the same gray level.
- ❖ Neighborhood gray tone difference matrix (NGTDM) (36): calculates the difference between a pixel's gray level and the average gray level of neighboring pixels. Key texture features include entropy, mean, directionality, roughness, and busyness.
- ❖ Gray level dependence matrix (GLDM): describes the gray level relationship between the central pixel and its surrounding domain pixels (37). Similar to GLSZM but with a restriction on the distance between neighboring pixels.

Higher-order features

Higher-order features generally involve using filter transforms to extract relevant features from an image. Filter-based feature extraction (38) is commonly employed to enhance features such as texture, edge, shape.

- ❖ Edge detection filters: (e.g., Sobel, Prewitt, Canny) identify the edges of the heart and blood vessels in MRI images, aiding in the segmentation of cardiac structures such as ventricular and atrial walls.
- ❖ Texture filters: (e.g., Gabor, Haralick, Marr-Hildreth) extract the texture features of cardiac tissues in MRI images, helping to differentiate various cardiac tissue types, such as myocardium, fat, and vessel walls.
- ❖ Scale-space filters: (e.g., Gaussian pyramid) facilitates the smoothing of MRI images at different scales and the extraction of multi-scale cardiac structural features.
- ❖ Frequency-domain filters: (e.g., Fourier or wavelet

transform) enable the conversion of cardiac MRI images from the image domain to the frequency domain, aiding in the extraction of frequency features, such as heartbeat cycles.

Feature engineering

Feature engineering (5) encompasses feature selection and dimensionality reduction techniques, aim to eliminate redundant features that may lead to model overfitting, identify the optimal set of radiomics features for modeling, and prevent feature correlations from impacting analysis results. This ensures the model's robust generalization performance during both internal validation and external testing.

(I) Feature selection (39) is categorized into three methods:
  (i) Filtering: this method scores each feature based on its relevance or significance, retaining those with higher relevance to the target variable. Standard techniques include the Pearson correlation coefficient, chi-square test, and mutual information.
  (ii) Wrapping: this approach typically employs machine learning algorithms such as random forest (RF), support vector machine (SVM) (40). It trains the model on various feature subsets using cross-validation or other validation methods, ultimately selecting the subset that performs best in internal validation and external testing.
  (iii) Embedding: this method integrates feature selection into the model's training process. It involves obtaining weight coefficients of each feature and selecting features based on these coefficients, usually employing techniques such as the L1 regularization penalty.

(II) Dimensionality reduction involves decreasing the number of data features. Common methods include:
  (i) Principal component analysis (PCA) (41): PCA uses linear transformations to covert the original n-dimensional feature space to a k-dimensional space. The resulting k-dimensional variables, known as principal components, recombine correlated features into a smaller set of uncorrelated new features.
  (ii) T-distributed stochastic neighborhood embedding (T-SNE) (42), initially intended for data visualization in low latitude space, T-SNE is a nonlinear dimensionality reduction technique. It maps high-dimensional data into a low-dimensional space (usually 2 or 3 dimensions) while preserving local dataset characteristics.

The goal of dimensionality reduction is to maintain as much of the original image information as possible while reducing computational complexity and mitigating the effects of the curse of dimensionality.

Model construction

Once features have been selected and dimensionality reduced, the data can be modeled using two common methods:

(I) Traditional machine learning: RF (43) is an ensemble learning method that combines multiple decision trees for classification and regression tasks. It works by aggregating the predictions of individual trees to improve accuracy and robustness. SVM (44) is a classical algorithm for binary and multiple classification. SVM works by identifying an optimal hyperplane to separates different classes sample points. It is also applicable to regression tasks, where it minimizes the distance between sample points.

(II) Deep learning: the convolutional neural networks (CNNs) (45) has emerged as a prominent model, known for their multi-level feature extraction capability. They excel at automatically learning and extracting abstract features from raw data, reducing the need for manual feature engineering (46). Through multi-level convolution and pooling operations, CNN can effectively capture high-level abstract features in data such as cardiac MRI images, allowing them to perform complex data modeling and classification tasks quickly and efficiently.

In MRI radiomics, these methods can be employed to classify cardiac diseases for example myocardial infarction, cardiomyopathy, and to predict cardiac functional features such as ventricular volume and ejection fraction (47).

Model validation is essential to assess the model's performance and generalization ability with new data:

(I) Hold-out: for large datasets, the hold-out method divides the dataset into a training set and a test set, typically with a ratio of 7:3 or 8:2. The model is trained on the training set and assessed on the test set, using metrics such as sensitivity, specificity, receiver operating characteristic (ROC) curve.

(II) Cross-validation: for small datasets, cross-validation divides the dataset into k subsets to fully utilize the data. One subset is used as the validation set, and the rest as the training set. This process is repeated k times, each time with a different validation set, and the average performance metrics are calculated.

In cases of dataset imbalance (e.g., low sample size for certain heart disease categories), stratified sampling is crucial to maintain appropriate representation of each category in both the training and test sets.

Statistical analysis

Statistical analysis plays a crucial role in processing and interpreting imaging data and model results in radiomics. Various statistical methods are employed to summarize, analyze, and interpret the statistical significance of data features and model outcomes, yielding meaningful information for disease diagnosis and treatment.

Descriptive statistical analysis

Involves data characteristics, such as mean, standard deviation, maximum and minimum values. This analysis helps understand the overall distribution of imaging data and compares model results.

Analysis of variance (ANOVA)

Used to compare differences between multiple groups. It can identify differences in the image features between different case or treatment groups, helping to pinpoint disease-related image features. In modeling, ANOVA can compare the generalization performance of models across different datasets.

Regression analysis

Models the association between an imaging feature and a target variable, such as disease risk or prognosis. It helps predict a patient's risk of disease or treatment outcome.

Reasonable statistical analysis of imaging data and experimental results is essential for identifying disease-related imaging features, optimizing disease diagnosis and treatment strategies, and enhancing the application value of medical imaging.

Cardiac MRI radiomics in non-ischemic cardiomyopathy

Non-ischemic cardiomyopathies, diverse in origin, are linked to disturbances in the heart's mechanical and electrical activity. These conditions are typically characterized by ventricular hypertrophy or dilatation, not attributable to pressure or volume overload or coronary artery disease (CAD), and often lead to cardiac death or dysfunction with progressive heart failure. Non-ischemic cardiomyopathies can be categorized into genetic (HCM, arrhythmogenic right ventricular cardiomyopathy), mixed (genetic and acquired DCM), and acquired (myocarditis) (48). This section focuses on the clinical applications of radiomics in the diagnosis and management of HCM, DCM, and myocarditis, the three most typical non-ischemic cardiomyopathies. Myocardial biopsy and cardiac MRI are the primary diagnostic tools for cardiomyopathy. Given the invasive nature of myocardial biopsy, MRI has become the essential, non-invasive diagnostic tool for non-ischemic cardiomyopathy.

MRI facilitates the non-invasive evaluation of cardiac structural, functional, and vascular abnormalities, including the evaluation of cardiac chamber morphology and function, myocardial tissue properties, perfusion, and microcirculatory dysfunction (49). However, challenges arise when using MRI as the sole diagnostic modality for cardiomyopathy. For instance, MRI cine sequences from patients with HCM and hypertensive cardiomyopathy (HHD) may both indicate left ventricle (LV) myocardial hypertrophy and could be negative for LGE. However, the T1 mapping values in these conditions may be similar, which is not consistent with the expected results (50) and can be misleading as they do not accurately reflect the distinct pathological process. In HCM, an increase in focal and diffuse collagen fiber deposition is anticipated, whereas in HHD, the findings are attributed to cardiomyocyte hypertrophy. The study (51) has shown that T1 mapping in LGE (–) HCM patients is comparable to that of normal healthy volunteers, resulting in an inability to make a diagnosis based on a single MRI sequence. These findings highlight the need for further technological advancements in cardiac MRI to improve its diagnostic accuracy.

The advancement of radiomics have shown promise in enhancing the diagnostic capabilities of cardiac MRI. Numerous studies (52,53) have demonstrated the potential of integrating cardiac MRI with radiomics to identify differences between diseases and various subtypes within the same disease (54). *Table 4* outlines the demographic characteristics, radiomic features, and associated tools of radiomics in different cardiac MRI sequences, such as T1 mapping, LGE, and cine, for typical non-ischemic

Table 4 Clinical applications of radiomics in different MRI sequences of non-ischemic cardiomyopathies, radiomics characterization, and related tools

Disease	Sequence	References	Patients	Age† (years)	Male, n [%]	Populations	Radiomic features	Radiomic tools
HCM	T1 mapping	Neisius *et al.* (55)	232	55±14	166 [72]	HCM, HHD, healthy	TA: histogram, run-length matrix, co-occurrence matrix, LBP	ROI selection: manually; feature extraction: MATLAB; data analysis: SPSS
	LGE	Fahmy *et al.* (56)	1,229	52±16	766 [62]	HCM, SCD	TA: histogram, cooccurrence matrix, size zone matrix, run length matrix, gray tone matrix, dependence matrix	ROI selection: manually; feature extraction: pyradiomics; data analysis: Python, R, MATLAB
	Cine	Pu *et al.* (57)	273	55	183 [67.54]	HCM	The maximal wall thickness slice and the entire left ventricular myocardium	ROI selection: manually segmented by ITK-SNAP; feature extraction: pyradiomics; data analysis: SPSS, R
DCM	T1 mapping	El-Rewaidy *et al.* (58)	321	55±15	225 [70]	DCM, HCM, healthy	TA: histogram-based features, GLRLM, GLCM, LBP	ROI selection: manually; feature extraction: MATLAB; data analysis: SPSS, MATLAB
	LGE	Shu *et al.* (59)	114	47.5	77 [67.5]	DCM	TA: GLCM contrast, GLCM difference average, GLCM difference entropy	ROI selection: manually drawn by CVI42; feature extraction: pyradiomics; data analysis: SPSS
	Cine	Zhang *et al.* (60)	283	–	–	DCM, HCM, healthy	TA: Gini index, relief, information gain, gain ratio, Euclidean distance, FAOV, mutual information maximization, and joint mutual information	ROI selection: manually; feature extraction: pyradiomics; data analysis: SPSS
Myocarditis	T1 mapping	Baessler *et al.* (61)	39	34.7±12.2	–	Myocarditis, healthy	TA: T2 run-length nonuniformity and T2 gray-level nonuniformity	ROI selection: manually drawn by MaZda; feature extraction: MaZda; data analysis: R
	LGE	Di Noto *et al.* (62)	173	MI: 66±9; myocarditis: 39±15	MI: 99 [94] myocarditis: 54 [87]	MI, myocarditis	TA, shape, and first-order descriptors	ROI selection: manually drawn by 3DSlicer; feature extraction: pyradiomics; data analysis: N/A

†, data are presented as median or mean ± standard deviation. SPSS, Statistical Package for the Social Sciences; CVI42 and ITK-SNAP are software tools used for medical image analysis. HCM, hypertrophic cardiomyopathy; HHD, hypertensive cardiomyopathy; SCD, sudden cardiac death; DCM, dilated cardiomyopathy; TA, texture analysis; LBP, local binary patterns; ROI, region of interest; LGE, late gadolinium enhancement; GLRLM, gray-level run-length matrix; GLCM, gray-level co-occurrence matrix; MI, myocardial infarction; N/A, not applicable; MRI, magnetic resonance imaging.

cardiomyopathy. Despite variations in MRI equipment, magnetic field strength, imaging parameters, and gadolinium dose across institutions, radiomics can extract and analyze multiple features from cardiac MRI images, yielding results that are independent of these factors (30). The radiomics process is generalizable: parameters set for one study are generally typically apply to others. For example, radiomics parameters used for 1.5T cardiac MRI images of Siemens can also be applicable to 3.0T images from Philips and General Electric, underscoring its versatility as a multimodal technique (63). It is important to note, however, that preprocessing steps required may vary. Since each study has a unique ROI and focuses on different features, researchers often adjust radiomics parameters to optimize experimental outcomes.

HCM

HCM is a prevalent genetic cardiomyopathy occurring in 1 out of every 500 individuals. It is characterized by diverse phenotypes, microvascular dysfunction, and myocardial fibrosis (64). MRI of HCM typically shows asymmetric ventricular hypertrophy, patchy or punctate foci of high-delayed enhancement in the mid-myocardium, and elevated global T1 mapping (65,66). Differentiating between concentric HCM, HHD, and exercise-induced cardiac hypertrophy poses a diagnostic challenge because all three conditions can exhibit left ventricular hypertrophy with positive delayed enhancement. Although T1 mapping can help differentiate among these conditions (50,67), the overlap in T1 mapping values can complicate its practical clinical application.

Radiomics is particularly well-suited for diagnosing HCM due to its robust generalization capabilities. Radiomics-based T1 mapping, incorporating histogram and texture analysis, has shown promise in distinguishing HCM patients from healthy volunteers and those with HHD, cardiac amyloidosis, left heart insufficiency, and DCM (68). In a study by Neisius *et al.* (55), 232 patients were classified into HCM and HHD groups and six texture features from T1 mapping images were identified that effectively differentiated between HHD and HCM. The diagnostic accuracy of the texture features reached a maximum of 86.2% [95% confidence interval (CI): 0.769 to 0.903], with a validation set accuracy of 80% (95% CI: 0.77 to 1.00). In contrast, the diagnostic accuracy of the global native T1 mapping in distinguishing between the two was 64% (95% CI: 0.452 to 0.640). Therefore, radiomics analysis of native T1 images can differentiate between these diseases more accurately than conventional global T1 mapping. Additionally, it has been shown (54) that radiomics analysis using native T1 mapping can distinguish β-myosin heavy chain- and β-myosin-binding protein C- associated HCM.

LGE is a strong predictor of sudden cardiac death (SCD) in patients with HCM. A study by Fahmy *et al.* (56), involving 1,229 HCM patients for 4 years, found that myocardial LGE radiomics strongly correlates with SCD risk and enhances the prognostic value of current ESC or AHA/ACC risk models.

HCM diagnosis often relies on a positive LGE or T1 mapping, but LGE requires gadolinium contrast injection, which poses potential risks to the patient's brain and kidneys. Recent research by Pu *et al.* (57), indicates that certain diagnostic assessments can be made using cine imaging alone, without LGE. In their study, 273 HCM patients were divided into validation and test sets in a 7:3 ratio. They extracted two radiomics features: maximum ventricular wall thickness slices and entire left ventricular myocardium to create five predictive models. In the validation set, the model based on the whole left ventricular myocardium demonstrated superior diagnostic performance, with an area under curve value (0.898), diagnostic accuracy (89.02%), sensitivity (92.54%), and F1 score (93.23%) in LGE-positive patients. The predictive model, incorporating whole left ventricular myocardium images and radiological features, shown strong diagnostic performance, robustness, and clinical application value. Additionally, Zhang *et al.* (69) demonstrated that integrating cine-cardiac MRI radiomic features with established predictive indicators can effectively identify HCM patients at an elevated risk of developing heart failure. This suggests that radiomics can serve as a complementary tool to traditional cardiac MRI analysis for HCM patients, with cine imaging providing a valuable diagnostic complement (70) to LGE in the comprehensive evaluation of left ventricular function and structure.

DCM

DCM is characterized by abnormal ventricular dilation and systolic dysfunction, evidenced by an abnormal left ventricular ejection fraction, without the presence of CAD or abnormal loading conditions. DCM can have both genetic and non-genetic causes, including drugs, toxins, and other cardiomyopathies (71). Early stages of DCM are often asymptomatic, but advanced DCM can manifest as heart failure, posing life-threatening risks (72). MRI in

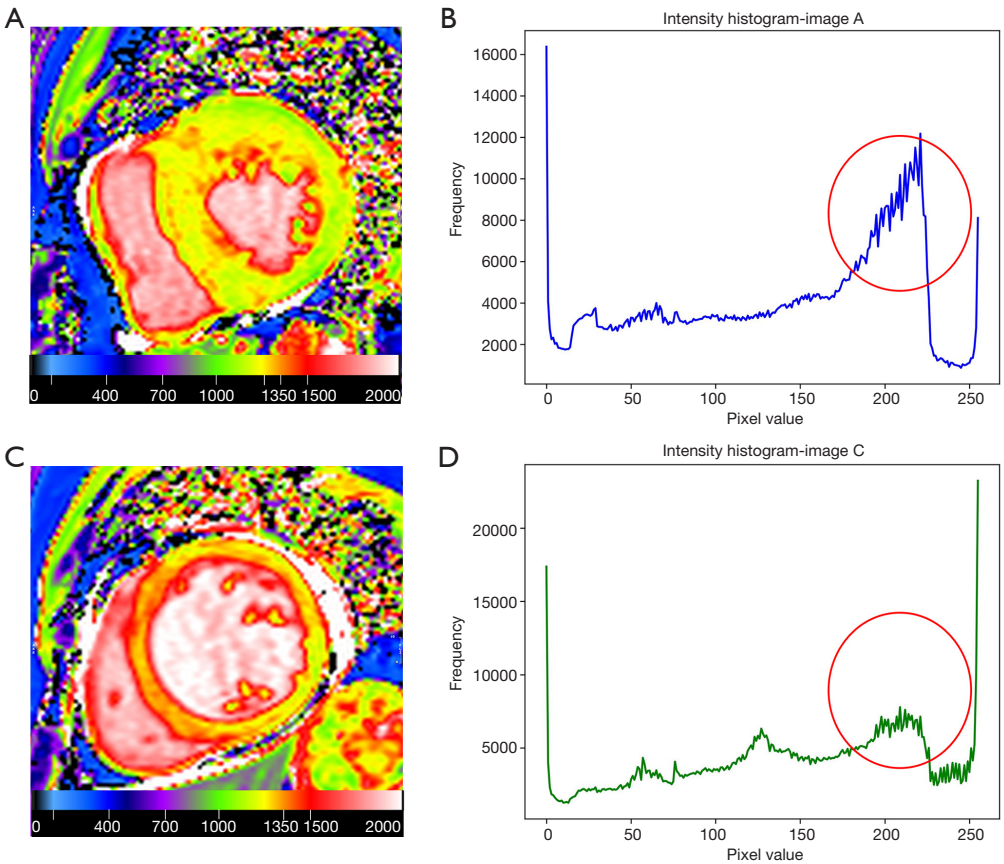

Figure 3 An example of radiomics applications: native T1 values and their corresponding radiomics gray intensity features in hypertrophic and dilated cardiomyopathy, highlighting distinct radiomic differences despite similar T1 values. (A) Native T1 value of hypertrophic cardiomyopathy: 1,237±62 ms; (B) corresponding radiomics gray intensity feature of (A); (C) native T1 value of dilated cardiomyopathy: 1,310±62 ms; (D) corresponding radiomics gray intensity feature of (C). Red circles in (B) and (D) highlight the distinct radiomic gray intensity features between (A) and (C), despite their native T1 value resemblance.

DCM typically reveals ventricular enlargement, reduced ejection fraction, and foci of LGE in the middle layers of the myocardial ventricular wall.

T1 mapping is crucial in diagnosing, treatment, and predicting prognosis of DCM patients. However, the native T1 and extracellular volume fraction (ECV) values in DCM and HCM are often similar (73), making it challenging to distinguish between these two diseases using T1 mapping alone. Radiomics, which can extract both superficial and deep features from images, is well-suited for this clinical situation (*Figure 3*). The study (58) has shown that texture analysis of myocardial native T1 mapping can differentiate different fibrosis patterns in DCM and HCM. Additionally, radiomics of native T1 has been shown to predict adverse cardiovascular events in patients with non-ischemic cardiomyopathies undergoing left ventricular reverse remodeling (74), as well as the likelihood of cardiac transplantation and all-cause mortality (75), outperforming conventional native T1 in these predictive roles. Recent study has demonstrated that radiomics extracted from T1 mapping and LGE can identify extracellular matrix components and subtle chronic inflammation in DCM (76).

LGE is an independent prognostic factor for adverse cardiovascular outcomes in DCM. Shu *et al.* (59) applied radiomics to LGE analysis in 114 DCM patients with severely reduced left ventricular ejection fraction <35%. The study extracted texture features from LGE images and followed up on outcomes such as heart transplantation and all-cause mortality. The findings showed that three texture features from the GLCM were significantly ($P<0.05$) associated with adverse outcomes, indicating their potential as independent prognostic factors. Therefore,

texture analysis of LGE emerges as a novel marker for risk stratification in DCM with severe LV systolic dysfunction.

Radiomics applied to cardiac cine sequences presents an effective method for distinguishing DCM from other diseases and healthy individuals. Zhang *et al.* (60) utilized ten feature selection methods for the left and right ventricles, and myocardium for DCM, HCM, and healthy individuals. They combined these features with nine classical machine learning methods based on the cardiac MRI radiomics, achieving an accuracy rate of 91.2%. Additionally, cine sequence-based radiomics can differentiate between DCM, left ventricular noncompaction, HCM, and healthy individuals (53). Differentiating between ischemic cardiomyopathy and DCM using cine sequences can be challenging for clinicians. However, Deng *et al.* (77) have shown that by integrating radiomic analysis with machine learning techniques in cine-cardiac MRI, it is feasible to distinguish DCM from ischemic cardiomyopathy. This approach minimizes the need for invasive diagnostic procedures and expedites the diagnostic process.

Myocarditis (inflammatory cardiomyopathy)

Myocarditis (78), an inflammatory myocardial disease caused by viral infections, drugs, toxins, or autoimmune inflammation, is a leading cause of heart failure, chronic DCM, and SCD. While myocardial biopsy is the gold standard for diagnosing myocarditis, its invasive nature and low sensitivity limit its clinical application. MRI enables the non-invasive diagnosis of suspected myocarditis and offers prognostic information for confirmed cases, making it an important assessment tool. The 2018 Lake Louise Criteria (LLC) (79) for cardiac MRI in myocarditis state that a diagnosis is made when at least one of the following criteria is met: (I) increase T2-weighting or T2 mapping in the global or localized myocardium; and (II) increased T1 mapping, ECV, LGE. High diagnostic performance is achieved if both are satisfied, but specificity is low if only one criterion is satisfied.

Radiomics has shown promise in diagnosing myocarditis. Texture analysis of T1 and T2 mapping in cardiac MRI can characterize different types of myocarditis with high sensitivity and specificity, serving as a complementary diagnostic tool to LLC. In a study by Baessler *et al.* (61), 39 patients with acute myocarditis with clinically suspected acute infarct-like myocarditis underwent MRI, endomyocardial biopsy, and cardiac catheterization. The study found that texture features, such as T2 gray-level nonuniformity and run-length nonuniformity, demonstrated superior diagnostic performance compared to mean T1, T2 values and LLC. In another study by the same group (80), 71 myocarditis patients exhibiting with symptoms of heart failure underwent myocardial biopsies, and texture analysis on T1 and T2 mapping images confirmed that radiomics-based texture analysis can be used as a complementary diagnostic tool in myocarditis.

Differentiating myocarditis from CAD using MRI is challenging because patients with myocarditis often present with chest pain similar to CAD, and atypical foci of LGE in myocarditis can appear subendocardial, resembling CAD manifestations. However, radiomics can help differentiate between myocardial infarction and myocarditis. In a study by Di Noto *et al.* (62), 111 patients with myocardial infarction and 62 patients with myocarditis underwent MRI. Features extracted from LGE images for texture, shape, and classificatory were analyzed by two independent physicians. The study concluded that LGE-based radiomics demonstrated high precision in differentiating myocardial infarction from myocarditis, correlating well with the subjective analyses by experienced physicians.

The application of radiomics in myocarditis is still emerging, with limited evidence available and requiring further evaluation. The lower prevalence of myocarditis compared to other diseases likely contributes to the scarcity of databases. However, current evidence suggests that radiomics can improve the diagnosis of myocarditis and effectively differentiate it from myocardial infarction (62).

Strengths and limitations

This review provides a comprehensive and standardized workflow for the application of radiomics to non-ischemic cardiomyopathies, which can serve as a practical guide for clinicians. By incorporating a detailed analysis of various cardiac MRI sequences and their specific roles in feature extraction, the review enhances the understanding of radiomics in cardiac imaging. Furthermore, the study bridges the gap between advanced imaging techniques and clinical practice, offering insights into how radiomics can aid in differentiating complex cardiac conditions. The inclusion of expert discussions serves to reinforce the relevance and applicability of the findings to real-world clinical scenarios.

Although this review offers a valuable framework for radiomics application, it is constrained by its reliance on existing studies that may not fully encompass all emerging

advancements in cardiac imaging. Additionally, the review primarily focuses on non-ischemic cardiomyopathies, and thus, the applicability to ischemic heart diseases remains unexplored. Furthermore, the absence of large-scale, multi-center validation studies limits the generalizability of the proposed workflow across different clinical settings. It is therefore necessary for future research to refine the algorithms, enhance image acquisition techniques and validate the proposed approaches in broader patient populations.

Conclusions

In summary, our review highlights the transformative potential of radiomics in medical imaging, particularly for diagnosing non-ischemic cardiomyopathies. We have delineated a comprehensive workflow for radiomics, encompassing the acquisition of cardiac MRI images across various sequences, followed by feature extraction, feature engineering, model construction, and data analysis. This workflow serves as a guide for implementing radiomics in both clinical and research settings, with the aim of improving diagnostic accuracy and supporting the future integration of radiomics into personalized cardiac care. By standardizing these techniques, we seek to promote greater inter-institutional comparability and facilitate data sharing, thereby enriching collective efforts in managing cardiac conditions. Moving forward, we recommend that future research focuses on multi-center validation studies, leveraging technological advancements in image acquisition, and refining algorithms to further optimize the use of radiomics in enhancing cardiac diagnostics and treatment.

Acknowledgments

We would like to express our sincere gratitude to all colleagues who provided valuable insights, feedback, and assistance in polishing this manuscript.
Funding: This study was supported by the National Natural Science Foundation of China (No. 82070426), the Natural Science Foundation of Hunan Province, China (No. 2022JJ50106), and the Department of Education of Hunan Province (No. HNJG-20230599).

Footnote

Reporting Checklist: The authors have completed the Narrative Review reporting checklist. Available at https://cdt.amegroups.com/article/view/10.21037/cdt-24-138/rc

Peer Review File: Available at https://cdt.amegroups.com/article/view/10.21037/cdt-24-138/prf

Conflicts of Interest: All authors have completed the ICMJE uniform disclosure form (available at https://cdt.amegroups.com/article/view/10.21037/cdt-24-138/coif). The authors have no conflicts of interest to declare.

Ethical Statement: The authors are accountable for all aspects of the work in ensuring that questions related to the accuracy or integrity of any part of the work are appropriately investigated and resolved.

References

1. Benz DC, Gräni C, Antiochos P, et al. Cardiac magnetic resonance biomarkers as surrogate endpoints in cardiovascular trials for myocardial diseases. Eur Heart J 2023;44:4738-47.
2. Karur GR, Aneja A, Stojanovska J, et al. Imaging of Cardiac Fibrosis: An Update, From the AJR Special Series on Imaging of Fibrosis. AJR Am J Roentgenol 2024;222:e2329870.
3. Korosoglou G, Sagris M, André F, et al. Systematic review and meta-analysis for the value of cardiac magnetic resonance strain to predict cardiac outcomes. Sci Rep 2024;14:1094.
4. Cadour F, Quemeneur M, Biere L, et al. Prognostic value of cardiovascular magnetic resonance T1 mapping and extracellular volume fraction in nonischemic dilated cardiomyopathy. J Cardiovasc Magn Reson 2023;25:7.
5. Wang YJ, Yang K, Wen Y, et al. Screening and diagnosis of cardiovascular disease using artificial intelligence-enabled cardiac magnetic resonance imaging. Nat Med 2024;30:1471-80.
6. Raisi-Estabragh Z, Izquierdo C, Campello VM, et al.

Cardiac magnetic resonance radiomics: basic principles and clinical perspectives. Eur Heart J Cardiovasc Imaging 2020;21:349-56.
7. Baeßler B, Engelhardt S, Hekalo A, et al. Perfect Match: Radiomics and Artificial Intelligence in Cardiac Imaging. Circ Cardiovasc Imaging 2024;17:e015490.
8. Shur JD, Doran SJ, Kumar S, et al. Radiomics in Oncology: A Practical Guide. Radiographics 2021;41:1717-32.
9. Raisi-Estabragh Z, Salih A, Gkontra P, et al. Estimation of biological heart age using cardiovascular magnetic resonance radiomics. Sci Rep 2022;12:12805.
10. Raisi-Estabragh Z, Jaggi A, Gkontra P, et al. Cardiac Magnetic Resonance Radiomics Reveal Differential Impact of Sex, Age, and Vascular Risk Factors on Cardiac Structure and Myocardial Tissue. Front Cardiovasc Med 2021;8:763361.
11. Polidori T, De Santis D, Rucci C, et al. Radiomics applications in cardiac imaging: a comprehensive review. Radiol Med 2023;128:922-33.
12. Stojanovska J, Feng L, Gilani N. Editorial for "Liver T1 Mapping Derived From Cardiac Magnetic Resonance Imaging: A Potential Prognostic Marker in Idiopathic Dilated Cardiomyopathy". J Magn Reson Imaging 2024;60:686-7.
13. Russo V, Lovato L, Ligabue G. Cardiac MRI: technical basis. Radiol Med 2020;125:1040-55.
14. Dux-Santoy L, Rodríguez-Palomares JF, Teixidó-Turà G, et al. Three-dimensional aortic geometry mapping via registration of non-gated contrast-enhanced or gated and respiratory-navigated MR angiographies. J Cardiovasc Magn Reson 2024;26:100992.
15. Rajiah PS, François CJ, Leiner T. Cardiac MRI: State of the Art. Radiology 2023;307:e223008.
16. Hesse K, Khanji MY, Aung N, et al. Assessing heterogeneity on cardiovascular magnetic resonance imaging: a novel approach to diagnosis and risk stratification in cardiac diseases. Eur Heart J Cardiovasc Imaging 2024;25:437-45.
17. Chen T, Ma KK, Chen LH. Tri-state median filter for image denoising. IEEE Trans Image Process 1999;8:1834-8.
18. Buades A, Coll B, Morel JM. A non-local algorithm for image denoising. 2005 IEEE Computer Society Conference on Computer Vision and Pattern Recognition (CVPR'05)2005. p. 60-5.
19. Nowak RD. Wavelet-based Rician noise removal for magnetic resonance imaging. IEEE Trans Image Process 1999;8:1408-19.
20. Bao LJ, Zhu YM, Liu WY, et al. Denoising human cardiac diffusion tensor magnetic resonance images using sparse representation combined with segmentation. Phys Med Biol 2009;54:1435-56.
21. Zhao M, Wei Y, Wong KKL. A Generative Adversarial Network technique for high-quality super-resolution reconstruction of cardiac magnetic resonance images. Magn Reson Imaging 2022;85:153-60.
22. Priya S, Dhruba DD, Sorensen E, et al. ComBat Harmonization of Myocardial Radiomic Features Sensitive to Cardiac MRI Acquisition Parameters. Radiol Cardiothorac Imaging 2023;5:e220312.
23. Lin K, Sarnari R, Carr JC, et al. Cine MRI-Derived Radiomics Features of the Cardiac Blood Pool: Periodicity, Specificity, and Reproducibility. J Magn Reson Imaging 2023;58:807-14.
24. Otsu N. A Threshold Selection Method from Gray-Level Histograms. IEEE Transactions on Systems, Man, and Cybernetics 1979;9:62-6.
25. Adams R, Bischof L. Seeded region growing. IEEE Transactions on Pattern Analysis and Machine Intelligence 1994;16:641-7.
26. Li C, Xu C, Gui C, et al. Level set evolution without re-initialization: a new variational formulation. 2005 IEEE Computer Society Conference on Computer Vision and Pattern Recognition (CVPR'05)2005. p. 430-6.
27. Bernard O, Lalande A, Zotti C, et al. Deep Learning Techniques for Automatic MRI Cardiac Multi-Structures Segmentation and Diagnosis: Is the Problem Solved? IEEE Trans Med Imaging 2018;37:2514-25.
28. Al-antari MA, Farea Shaaf Z, Mahadi Abdul Jamil M, et al. Deep learning myocardial infarction segmentation framework from cardiac magnetic resonance images. Biomedical Signal Processing and Control 2024;89.
29. Mayerhoefer ME, Materka A, Langs G, et al. Introduction to Radiomics. J Nucl Med 2020;61:488-95.
30. Zwanenburg A, Vallières M, Abdalah MA, et al. The Image Biomarker Standardization Initiative: Standardized Quantitative Radiomics for High-Throughput Image-based Phenotyping. Radiology 2020;295:328-38.
31. Whybra P, Zwanenburg A, Andrearczyk V, et al. The Image Biomarker Standardization Initiative: Standardized Convolutional Filters for Reproducible Radiomics and Enhanced Clinical Insights. Radiology 2024;310:e231319.
32. Durmaz ES, Karabacak M, Ozkara BB, et al. Radiomics-based machine learning models in STEMI: a promising tool for the prediction of major adverse cardiac events. Eur

Radiol 2023;33:4611-20.
33. Haralick RM, Shanmugam K, Dinstein IH. Textural Features for Image Classification. IEEE Transactions on Systems, Man, and Cybernetics 1973;SMC-3:610-21.
34. Galloway MM. Texture analysis using gray level run lengths. Computer Graphics and Image Processing 1975;4:172-9.
35. Thibault G, Angulo J, Meyer F. Advanced statistical matrices for texture characterization: application to cell classification. IEEE Trans Biomed Eng 2014;61:630-7.
36. Amadasun M, King R. Textural features corresponding to textural properties. IEEE Transactions on Systems, Man, and Cybernetics 1989;19:1264-74.
37. Wichtmann BD, Harder FN, Weiss K, et al. Influence of Image Processing on Radiomic Features From Magnetic Resonance Imaging. Invest Radiol 2023;58:199-208.
38. Huang S, Liu J, Lee LC, et al. An image-based comprehensive approach for automatic segmentation of left ventricle from cardiac short axis cine MR images. J Digit Imaging 2011;24:598-608.
39. Song J, Yin Y, Wang H, et al. A review of original articles published in the emerging field of radiomics. Eur J Radiol 2020;127:108991.
40. Attallah O, Ragab DA. Auto-MyIn: Automatic diagnosis of myocardial infarction via multiple GLCMs, CNNs, and SVMs. Biomedical Signal Processing and Control 2023;80.
41. Kamel M, Smith BT, Wahi G, et al. Continuous cardiometabolic risk score definitions in early childhood: a scoping review. Obes Rev 2018;19:1688-99.
42. Franco P, Sotelo J, Guala A, et al. Identification of hemodynamic biomarkers for bicuspid aortic valve induced aortic dilation using machine learning. Comput Biol Med 2022;141:105147.
43. Ma C, Luo G, Wang K. A Combined Random Forests and Active Contour Model Approach for Fully Automatic Segmentation of the Left Atrium in Volumetric MRI. Biomed Res Int 2017;2017:8381094.
44. Mantilla J, Garreau M, Bellanger J-J, et al. SVM-based classification of LV wall motion in cardiac MRI with the assessment of STE. 10th International Symposium on Medical Information Processing and Analysis: SPIE; 2015. p. 128-33.
45. Wu B, Fang Y, Lai X. Left ventricle automatic segmentation in cardiac MRI using a combined CNN and U-net approach. Comput Med Imaging Graph 2020;82:101719.
46. Jafari M, Shoeibi A, Khodatars M, et al. Automated diagnosis of cardiovascular diseases from cardiac magnetic resonance imaging using deep learning models: A review. Comput Biol Med 2023;160:106998.
47. Olaisen S, Smistad E, Espeland T, et al. Automatic measurements of left ventricular volumes and ejection fraction by artificial intelligence: clinical validation in real time and large databases. Eur Heart J Cardiovasc Imaging 2024;25:383-95.
48. McKenna WJ, Maron BJ, Thiene G. Classification, Epidemiology, and Global Burden of Cardiomyopathies. Circ Res 2017;121:722-30.
49. Guo R, Weingärtner S, Šiurytė P, et al. Emerging Techniques in Cardiac Magnetic Resonance Imaging. J Magn Reson Imaging 2022;55:1043-59.
50. Wu LM, An DL, Yao QY, et al. Hypertrophic cardiomyopathy and left ventricular hypertrophy in hypertensive heart disease with mildly reduced or preserved ejection fraction: insight from altered mechanics and native T1 mapping. Clin Radiol 2017;72:835-43.
51. Brouwer WP, Baars EN, Germans T, et al. In-vivo T1 cardiovascular magnetic resonance study of diffuse myocardial fibrosis in hypertrophic cardiomyopathy. J Cardiovasc Magn Reson 2014;16:28.
52. Wu CW, Wu R, Shi RY, et al. Histogram Analysis of Native T(1) Mapping and Its Relationship to Left Ventricular Late Gadolinium Enhancement, Hypertrophy, and Segmental Myocardial Mechanics in Patients With Hypertrophic Cardiomyopathy. J Magn Reson Imaging 2019;49:668-77.
53. Izquierdo C, Casas G, Martin-Isla C, et al. Radiomics-Based Classification of Left Ventricular Non-compaction, Hypertrophic Cardiomyopathy, and Dilated Cardiomyopathy in Cardiovascular Magnetic Resonance. Front Cardiovasc Med 2021;8:764312.
54. Wang J, Yang F, Liu W, et al. Radiomic Analysis of Native T(1) Mapping Images Discriminates Between MYH7 and MYBPC3-Related Hypertrophic Cardiomyopathy. J Magn Reson Imaging 2020;52:1714-21.
55. Neisius U, El-Rewaidy H, Nakamori S, et al. Radiomic Analysis of Myocardial Native T(1) Imaging Discriminates Between Hypertensive Heart Disease and Hypertrophic Cardiomyopathy. JACC Cardiovasc Imaging 2019;12:1946-54.
56. Fahmy AS, Rowin EJ, Jaafar N, et al. Radiomics of Late Gadolinium Enhancement Reveals Prognostic Value of Myocardial Scar Heterogeneity in Hypertrophic Cardiomyopathy. JACC Cardiovasc Imaging 2024;17:16-27.

57. Pu C, Hu X, Lv S, et al. Identification of fibrosis in hypertrophic cardiomyopathy: a radiomic study on cardiac magnetic resonance cine imaging. Eur Radiol 2023;33:2301-11.
58. El-Rewaidy H, Neisius U, Nakamori S, et al. Characterization of interstitial diffuse fibrosis patterns using texture analysis of myocardial native T1 mapping. PLoS One 2020;15:e0233694.
59. Shu S, Wang C, Hong Z, et al. Prognostic Value of Late Enhanced Cardiac Magnetic Resonance Imaging Derived Texture Features in Dilated Cardiomyopathy Patients With Severely Reduced Ejection Fractions. Front Cardiovasc Med 2021;8:766423.
60. Zhang X, Cui C, Zhao S, et al. Cardiac magnetic resonance radiomics for disease classification. Eur Radiol 2023;33:2312-23.
61. Baessler B, Luecke C, Lurz J, et al. Cardiac MRI Texture Analysis of T1 and T2 Maps in Patients with Infarctlike Acute Myocarditis. Radiology 2018;289:357-65.
62. Di Noto T, von Spiczak J, Mannil M, et al. Radiomics for Distinguishing Myocardial Infarction from Myocarditis at Late Gadolinium Enhancement at MRI: Comparison with Subjective Visual Analysis. Radiol Cardiothorac Imaging 2019;1:e180026.
63. Wennmann M, Rotkopf LT, Bauer F, et al. Reproducible Radiomics Features from Multi-MRI-Scanner Test-Retest-Study: Influence on Performance and Generalizability of Models. J Magn Reson Imaging 2024. [Epub ahead of print]. doi: 10.1002/jmri.29442.
64. Ommen SR, Ho CY, Asif IM, et al. 2024 AHA/ACC/AMSSM/HRS/PACES/SCMR Guideline for the Management of Hypertrophic Cardiomyopathy: A Report of the American Heart Association/American College of Cardiology Joint Committee on Clinical Practice Guidelines. Circulation 2024;149:e1239-311.
65. Xu J, Zhuang B, Sirajuddin A, et al. MRI T1 Mapping in Hypertrophic Cardiomyopathy: Evaluation in Patients Without Late Gadolinium Enhancement and Hemodynamic Obstruction. Radiology 2020;294:275-86.
66. Baxi AJ, Restrepo CS, Vargas D, et al. Hypertrophic Cardiomyopathy from A to Z: Genetics, Pathophysiology, Imaging, and Management. Radiographics 2016;36:335-54.
67. Swoboda PP, McDiarmid AK, Erhayiem B, et al. Assessing Myocardial Extracellular Volume by T1 Mapping to Distinguish Hypertrophic Cardiomyopathy From Athlete's Heart. J Am Coll Cardiol 2016;67:2189-90.
68. Zhang H, Tian J, Zhang C, et al. Discrimination models with radiomics features derived from cardiovascular magnetic resonance images for distinguishing hypertensive heart disease from hypertrophic cardiomyopathy. Cardiovasc Diagn Ther 2024;14:129-42.
69. Zhang H, Zhao L, Wang H, et al. Radiomics from Cardiovascular MR Cine Images for Identifying Patients with Hypertrophic Cardiomyopathy at High Risk for Heart Failure. Radiol Cardiothorac Imaging 2024;6:e230323.
70. Cau R, Pisu F, Pintus A, et al. Cine-cardiac magnetic resonance to distinguish between ischemic and non-ischemic cardiomyopathies: a machine learning approach. Eur Radiol 2024;34:5691-704.
71. Pinto YM, Elliott PM, Arbustini E, et al. Proposal for a revised definition of dilated cardiomyopathy, hypokinetic non-dilated cardiomyopathy, and its implications for clinical practice: a position statement of the ESC working group on myocardial and pericardial diseases. Eur Heart J 2016;37:1850-8.
72. Jefferies JL, Towbin JA. Dilated cardiomyopathy. Lancet 2010;375:752-62.
73. Messroghli DR, Moon JC, Ferreira VM, et al. Clinical recommendations for cardiovascular magnetic resonance mapping of T1, T2, T2* and extracellular volume: A consensus statement by the Society for Cardiovascular Magnetic Resonance (SCMR) endorsed by the European Association for Cardiovascular Imaging (EACVI). J Cardiovasc Magn Reson 2017;19:75.
74. Chang S, Han K, Kwon Y, et al. T1 Map-Based Radiomics for Prediction of Left Ventricular Reverse Remodeling in Patients With Nonischemic Dilated Cardiomyopathy. Korean J Radiol 2023;24:395-405.
75. Zhang J, Xu Y, Li W, et al. The Predictive Value of Myocardial Native T1 Mapping Radiomics in Dilated Cardiomyopathy: A Study in a Chinese Population. J Magn Reson Imaging 2023;58:772-9.
76. Nakamori S, Amyar A, Fahmy AS, et al. Cardiovascular Magnetic Resonance Radiomics to Identify Components of the Extracellular Matrix in Dilated Cardiomyopathy. Circulation 2024;150:7-18.
77. Deng J, Zhou L, Li Y, et al. Integration of Cine-cardiac Magnetic Resonance Radiomics and Machine Learning for Differentiating Ischemic and Dilated Cardiomyopathy. Acad Radiol 2024;31:2704-14.
78. Sagar S, Liu PP, Cooper LT Jr. Myocarditis. Lancet 2012;379:738-47.
79. Ferreira VM, Schulz-Menger J, Holmvang G, et al.

Cardiovascular Magnetic Resonance in Nonischemic Myocardial Inflammation: Expert Recommendations. J Am Coll Cardiol 2018;72:3158-76.
80. Baessler B, Luecke C, Lurz J, et al. Cardiac MRI and Texture Analysis of Myocardial T1 and T2 Maps in Myocarditis with Acute versus Chronic Symptoms of Heart Failure. Radiology 2019;292:608-17.

Cite this article as: Deng J, Zhou L, Liao B, Cai Q, Luo G, Zhou H, Tang H. Challenges in clinical translation of cardiac magnetic resonance imaging radiomics in non-ischemic cardiomyopathy: a narrative review. Cardiovasc Diagn Ther 2024;14(6):1210-1227. doi: 10.21037/cdt-24-138

